Splitting of polarization absorption bands with a complex vibron structure in the spectra of impurity liquid crystals

E. M. Aver'yanov, V. M. Muratov, V. G. Rumyantsev, and V. A. Churkina

Scientific-Research Institute of Organic Semiconductors and Dyes
(Submitted 7 June 1985; resubmitted 2 September 1985)
Zh. Eksp. Teor. Fiz. **90**, 100–110 (January 1986)

Strong splitting of the spectral bands of impurity liquid crystals has been discovered and investigated experimentally. The splitting is one or two orders of magnitude larger than hitherto observed and exceeds theoretical estimates of band shifts based on conventional mechanisms involving molecular interactions in liquid crystals. The impurity band splitting is related to the orientation order and polarity of the matrix and to perturbations of the electron structure of the impurity molecules in the mesophase. It is shown that specific features of vibron structure of the bands are responsible for the novel band-splitting mechanism. A method is proposed and tested for obtaining complete information on the polarization of intramolecular transitions, a theory of the band-splitting mechanism is developed, and the experimental results are interpreted quantitatively.

1. INTRODUCTION

Previous spectral studies of pure and (especially) impure liquid crystals (LC) have been concerned primarily with recording the positions of the electron absorption bands and measuring the relative dichroism $N = D_{\parallel}/D_{\perp}$, where $D_{\parallel}$ and $D_{\perp}$ are the optical densities for the polarizations along and normal to the director. These parameters determine the color and contrast properties of LC displays.[1] Little work has been done on the molecular electron structure or on the positions and shapes of the polarization bands during phase transitions in LC's, and this is particularly true with regard to theory.

The influence of static[2,3] and resonant[3–5] intermolecular interactions on the intensity, position, splitting, and shape of the LC absorption bands has been studied previously by drawing on the analogy with molecular crystals. Theoretical estimates for the band shifts and splittings in liquid crystals range from 10 to 100 cm^{-1} and agree with the experimental observations in Refs. 2, 6, and 7. Because the electron absorption bands in LC's are so wide (thousands of cm^{-1}), these effects are not accessible to detailed experimental analysis and cannot be used for practical applications.

This situation changed with the discovery of strong splitting (by $\sim 1000\ cm^{-1}$) of the polarization bands for absorption caused by impurity molecules (azulene derivatives) present in LC matrices.[8] Accurate measurements of the band splittings permitted a detailed experimental analysis of their relation to the molecular electron structure, the LC order, and the properties of the intermolecular interaction. However, the reasons for the strong splitting remained obscure. We previously detected and investigated perturbations of the electron structure for molecules of this type in an LC matrix.[9]

The goal of the present work is to experimentally study and theoretically interpret the shifts and splittings of the polarization absorption bands for azulene derivatives in LC matrices. The impurity molecules which we studied are described in Sec. 2, where the spectral data are analyzed and we show that the large observed splitting cannot be due to ordinary intermolecular interaction mechanisms but instead can be traced to the vibronic structure of the bands. In Sec. 3 we suggest a technique for studying the polarization of molecular transitions in terms of the temperature behavior of the relative dichroism $N = D_{\parallel}/D_{\perp}$ of the absorption bands. This method was tested experimentally for two of the impurity LC's. In Sec. 4 we analyze the temperature dependences of the splittings for LC matrices with different polarities, mesophase interval widths, and orientational order. The theory developed for the vibronic band-splitting mechanism is used to interpret the experimental results quantitatively.

2. IMPURITY LIQUID CRYSTALS AND THEIR SPECTRAL PROPERTIES

The nematic LC matrices consisted of a mixture of cyclohexane carbonates (CHC) and 4-*n*-pentyl-4′-cyanobiphenyl (5CB). The mesophase in CHC exists for temperatures in the interval $-27 \leqslant T \leqslant -92.5$ °C; CHC is transparent down to $\lambda \approx 200$ nm, is relatively nonpolar, and is only weakly birefringent. The 5CB matrix is in the nematic phase for $22.5 \leqslant T \leqslant 35$° C; it starts to absorb at $\lambda \approx 330$ nm and possesses a pronounced dielectric anisotropy and birefringence. The orientational order, the dispersion of the refractive indices, and the components of the Lorentz tensor for the CHC and 5CB matrices are needed to interpret the spectral data; we measured them previously in Ref. 9, 10, and 11 respectively.

The impurity concentration was low enough to keep resonant interactions from affecting the impurity absorption characteristics; resonant impurity-matrix interaction was not a factor either, because we studied the impurity bands at visible wavelengths far from the intrinsic absorption bands of the matrices. Because the refractive index n varied only slightly with wavelength near the impurity absorption band, the wavelength dependence of the local field did not have any influence on the splitting of the polarization impurity

 0038-5646/86/010057-06$04.00

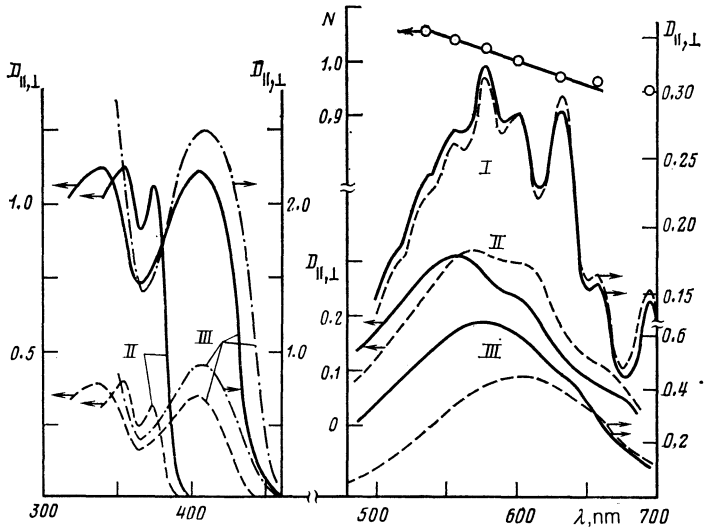

FIG. 1. Spectral dependence of the optical densities $D_{\parallel}$ (solid curves) and $D_{\perp}$ (dashed) for a CHC matrix ($T = 20$ °C) containing impurity molecules I (cell thickness $d = 60\,\mu$m, impurity concentration $c = 0.123$ moles/liter), II and III ($\lambda > 460$ nm, $d = 68\,\mu$m, $c = 0.137$ M). For $\lambda < 460$ nm, $d = 43\,\mu$m and $c = 0.028$ M for impurity II; for III in CHC, $d = 18\,\mu$m, $c = 0.021$ M; for III in 5CB (dashed-dotted curves, $T = 22$ °C), $d = 28\,\mu$m, $c = 0.21$ M. Upper right: spectral dependence of the dichroism $N = D_{\parallel}/D_{\perp}$ of the maxima of the vibronic bands in the first electron transition for impurity I.

bands. Thus, of the known mechanisms involving intermolecular interactions in these materials, only static impurity-matrix interactions seem capable of accounting for the observed splitting. This motivated our choice of the four impurity molecules with the structures shown below.

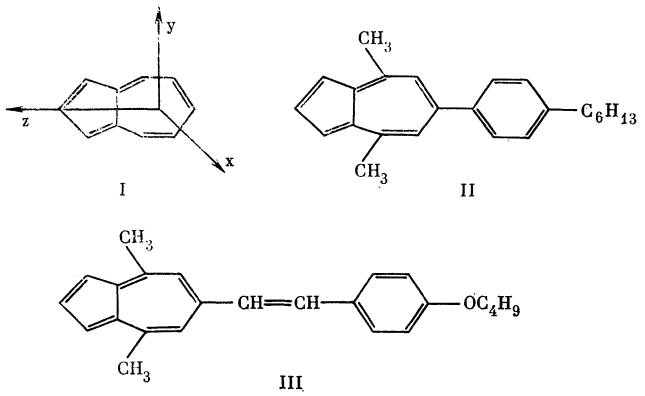

Figure 1 shows the absorption bands for the impurities I–III to be discussed in this paper. The wavelength and relative intensity of the vibron bands for the first electronic transition in azulene (I) in CHC agree closely with published data for azulene in isotropic solvents,[12] and the same is true for the triplet second-electronic-transition band ($\lambda_{max} = 352, 340, 325$ nm). The absorption bands for II and III are also due to the first electronic transition in azulene, but the substituents shift them to longer wavelengths.[9]

The vibronic structure of the azulene band shown in Fig. 1 consists of narrow, rather well-resolved peaks at wavelengths that are independent of the polarization ($\parallel,\perp$) and the phase of the matrix. This property is ideal for observing band shifts and splittings caused by static interaction between the impurity molecules and the matrix. According to Refs. 2 and 3, the magnitude of the static splitting increases with the dispersion

$$\Delta_p = \langle [P_2(\cos\theta) - S]^2 \rangle,$$

where $S = \langle P_2 \rangle = \langle 3\cos^2\theta - 1 \rangle/2$, θ is the angle between the long molecular axis and the LC director, and $\langle ... \rangle$ denotes a statistical average. Δ_p increases as the molecular geometry becomes more symmetric and as T approaches the phase transition temperature T_c at which the LC becomes an isotropic liquid.[13] We would therefore expect that the static band splitting should increase in the order III, II, I and as $T \to T_c$, but this contradicts the experimental results. Furthermore, if the transition dipole moment makes the "magic angle" $\beta = \beta_m = 54.7°$ with the long molecular axis, there is no static splitting of the absorption band.[3] We have $\beta \approx \beta_m$ for the maximum of band II (see below); however, the splitting for this band is quite large (both the maxima in the band and the centroids of the band components differ appreciably). Finally, if the components were shifted by static interaction, one would expect the inequalities $\lambda_{\parallel} > \lambda_{\perp} > \lambda_i$ to hold[2,3] for the centroids of the components for materials with $\beta < \beta_m$; however, one finds experimentally that $\lambda_{\perp} > \lambda_i > \lambda_{\parallel}$ for band III. The above analysis thus shows that static impurity-matrix interaction cannot be responsible for the splitting of bands II and III.

In order to ascertain if impurity complexation influenced the observed dichroism and splitting, we studied these characteristics as functions of the concentration of impurities II and III in LC matrices for $c = 10^{-1}$–10^{-4} mole/liter. We did not detect any change in N or $\Delta\lambda$. Moreover, an analysis of the absorption spectra for impurities in matrices of widely differing polarities showed that the splitting was insensitive to the polarity of the matrix. Finally, we note that the oscillator strengths for the long-wave transitions for I–III are small, as is the change in the azulene dipole moment during the transition to the first excited electron state.[12,14] These facts indicate that the intermolecular interactions do not contribute significantly to the observed splitting.

The dependence of the dichroism N of the azulene vibron bands on their spectral position (Fig. 1) indicates that the vibronic transitions have different polarizations with respect to the molecular axes. The "inversion" point, at which $N = 1$, is nearly equal to the wavelength corresponding to the absolute absorption maximum and with the centroid of the vibronic band series for I. The fine structure of the long-wave band for II and III is less well-defined than for I; however, the absolute absorption maximum again corresponds

to the fourth vibronic transition (just as for impurity I), in agreement with the data in Ref. 12, where other azulene derivatives were studied. The polarization of the vibronic transitions changes monotonically with λ, as can be seen from the monotonic dependence $N(\lambda)$ for band I, and this causes the absorption lineshapes for II and III to depend on the polarization of the light (parallel or normal to the director); the maxima and the centroids for the $\parallel$ and $\perp$ polarizations also differ. The vibronic structure and the ordered alignment of the impurity molecules in the LC matrix are resonsible for this novel intramolecular splitting mechanism, which will be analyzed systematically in the next section.

3. POLARIZATION OF THE INTRAMOLECULAR TRANSITIONS. DICHROISM

The experimental results discussed above, which indicate that the polarizations differ for the vibronic transitions in azulene, extend our knowledge regarding the electronic structure of this molecule.[12] We will show how to obtain complete information regarding the polarization of the intramolecular transitions.

We take the x, y, z axes for the stick-shaped molecules II and III to be as shown for the azulene moiety (Sec. 2); in a uniaxial LC, the molecular alignment with respect to these axes is described by the traceless diagonal matrix[1]

$$S_{ii}=\langle 3\cos^2\theta_{iz}-1\rangle/2, \quad i=x,\ y,\ z, \tag{c}$$

where θ_{iz} is the angle between the director Z and the i-axis of the molecule. If the molecular rotation about the z axis is impeded, the parameter $G\equiv S_{yy}-S_{xx}$ is nonzero. If we specify the polarization of the vibronic transition in the molecular coordinate system in terms of the polar and azimuthal angles β and φ, then the equations[9]

$$\begin{aligned} K\frac{n_\parallel}{\rho f_\parallel^2}D_\parallel=A_\parallel=\frac{A_n}{3}\left(1+2SS_\beta-\frac{2}{3}GG_{\beta\varphi}\right),\\ K\frac{n_\perp}{\rho f_\perp^2}D_\perp=A_\perp=\frac{A_n}{3}\left(1-SS_\beta+\frac{1}{3}GG_{\beta\varphi}\right),\\ K\frac{n_i}{\rho_i f_i^2}D_i=\frac{A_i}{3} \end{aligned} \tag{1}$$

relate the experimentally measured optical densities $D_{\parallel,\perp}$ (in the uniaxial LC) and D_i (in the isotropic liquid) to the corresponding components $A_{\parallel,\perp,i}$ of the oscillator strength. Here $K=$ const, $S=S_{zz}$, and $n_{\parallel,\perp,i}$ are the background values of the refractive indices for wavelengths in the absorption band (for impurity absorption, they coincide with the refractive indices for the matrix); ρ and ρ_i are the densities of the nematic and isotropic phases; A_n and A_i are the oscillator strengths for the transition in the nematic and isotropic phases;

$$\begin{aligned} S_\beta=(3\cos^2\beta-1)/2, \quad G_{\beta\varphi}=(3\sin^2\beta\cos 2\varphi)/2,\\ f_{\parallel,\perp}=1+L_{\parallel,\perp}(n_{\parallel,\perp}^2-1) \end{aligned} \tag{2}$$

are the components of the local field tensor; $L_{\parallel,\perp}$ are the components of the Lorentz tensor.

The orientational order of the molecules and the polarization of the transition are characterized in the molecular coordinate system by the parameter

$$\Sigma=SS_\beta-{}^1/_3GG_{\beta\varphi}. \tag{3}$$

We can use (1) to relate Σ to the dichroism N of the band

$$\Sigma=\frac{Ng_i-1}{Ng_i+2}, \quad g_i=\frac{n_\parallel}{n_\perp}\left(\frac{f_\perp}{f_\parallel}\right)^2. \tag{4}$$

If S and G are fixed and we choose any three intramolecular transitions 1, 2, 3, Eq. (3) implies that

$$\Sigma(1)/\Sigma(3)=B\Sigma(2)/\Sigma(3)+C, \tag{5}$$

where

$$\begin{aligned} B=\frac{S_\beta(1)G_{\beta\varphi}(3)-G_{\beta\varphi}(1)S_\beta(3)}{S_\beta(2)G_{\beta\varphi}(3)-G_{\beta\varphi}(2)S_\beta(3)},\\ C=\frac{S_\beta(2)G_{\beta\varphi}(1)-G_{\beta\varphi}(2)S_\beta(1)}{S_\beta(2)G_{\beta\varphi}(3)-G_{\beta\varphi}(2)S_\beta(3)}. \end{aligned} \tag{6}$$

If the orientation of the transition moments relative to the molecular axes is independent of the temperature in the mesophase, the linear dependence (5) will hold for all temperatures in the mesophase interval, even though the order parameter Σ changes with temperature. In this case, if we know β and φ for two of the transitions and B and C in (6) have been measured experimentally, we can calculate β and φ for the third transition, i.e., obtain complete information about its polarization. The advantage of this technique is that one can combine parameter values Σ corresponding to various types of bands (vibrational, electronic, or vibronic intramolecular transitions). Moreover, the procedure is independent of the molecular structure. Since only the uniaxial symmetry of the mesophase was used to derive (5), either nematic or type-A smectic LC's can be used as the matrix.

Because the observed splittings for bands II and III are considerably less than the band halfwidths, the above approach can be used to analyze the polarization of the vibronic transitions corresponding to the band maxima. We choose bands 1, 2, and 3 in (5) to be the bands at $\lambda_{max}=373$, 355, and 567 nm for impurity II. The order parameters Σ for the first two transitions for II in CHC were found as functions of T in Ref. 9; Fig. 2 shows the temperature dependence

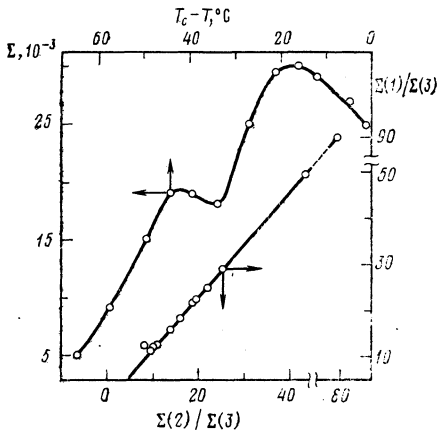

FIG. 2. Temperature dependence of Σ for the 567 nm band of impurity II in CHC, and the ratio $\Sigma(1)/\Sigma(3)$ as a function of $\Sigma(2)/\Sigma(3)$ for the transitions $\lambda_{max}=373$ (1), 355 (2), and 567 nm (3) for impurity II.

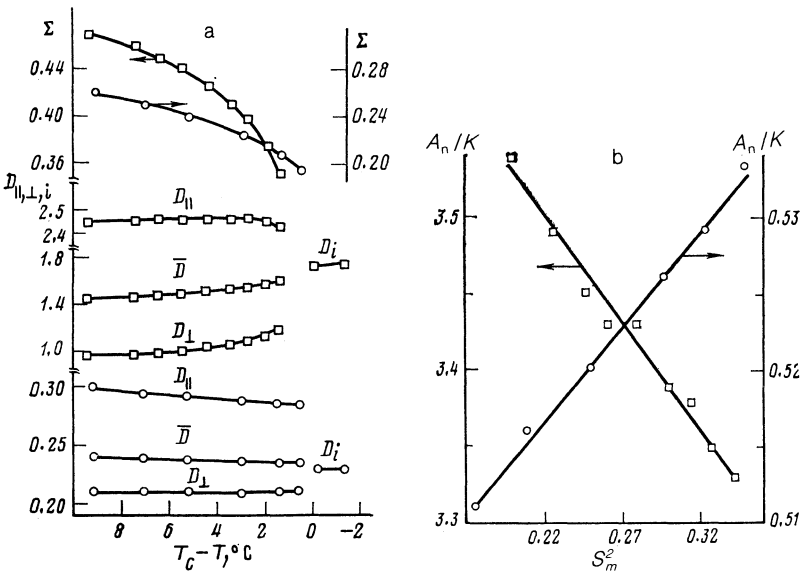

FIG. 3. Change in the spectral parameters of the bands at $\lambda_{max} = 407$ (□, $d = 28\ \mu$m, $c = 0.21$ M) and 580 nm (○, $d = 28\ \mu$m, $c = 0.134$ M) for impurity III in a 5CB matrix. a) Temperature dependences of Σ and the optical densities $D_{\|,\perp,i}$ of the matrix at wavelengths in the impurity absorption band. b) Reduced oscillator strengths A_n/K (7) for the electron transitions in III as functions of the order parameter S_m^2 for a 5CB matrix.

for $\Sigma(3)$. Although this dependence is complicated, the linear relation (5) holds with constant coefficients $B = 1.125$ and $C = 0.45$ throughout the mesophase interval and for a wide range of values $\Sigma(1)/\Sigma(3)$. This implies that the angles $\beta(3)$ and $\varphi(3)$ are independent of T in the mesophase. The 373 and 355 nm transitions are polarized along the z axis of the azulene moiety of II; moreover, for these long molecules S is $\geqslant G/3$ and we may neglect the contribution from the second term in the right-hand side of (3) for these transitions. Setting $S_\beta(1) = 1$, $G_{\beta\varphi}(1) = 0$, and estimating $S_\beta(2) \approx \Sigma(2)/\Sigma(1) \approx 0.87$ from the data in Ref. 9, we find from (6) that $\beta(3) = 53°$ and $\cos 2\varphi(3)/\cos 2\varphi(2) = -0.27$. Thus, $\varphi(3)$ changes from 53 to 37° as $\varphi(2)$ varies over its full range 0–90°, and the most likely value of $\varphi(3)$ is 45°($\pm$ 8°).

We established previously[9] that the linear dependence (5) (with constant coefficients $B = 1.28$ and $C = -0.56$) holds for the III impurity bands in CHC with $\lambda_{max} = 404(1)$, 340(2), and 590 nm(3). If we set $S_\beta(1) = 1$, $G_{\beta\varphi}(1) = 0$, and estimate $S_\beta(2) \approx \Sigma(2)/\Sigma(1) \approx 0.94$ from the data in Ref. 9, we find from (6) that $\beta(3) = 40°$ and $\cos 2\varphi(3)/\cos 2\varphi(2) = 0.21$. The interval $0 \leqslant \varphi(2) \leqslant 90°$ corresponds to $39 \leqslant \varphi(3) \leqslant 51°$, i.e., the most probable value is $\varphi(3) = 45 \mp 6°$.

We thus see that because of the longer chain of π-conjugate electrons in the aromatic core of derivative III, the orientation of its vibronic transition moment corresponding to the peak of the longwave absorption band is quite different than for molecule II. The change in β is the primary factor determining the difference in the dichroism for II and III, since we have $\varphi \approx 45°$ and $G_{\beta\varphi} \approx 0$ for both molecules. This can be clearly seen from Fig. 1, where $N \lesssim 1$ for band II and $N > 1$ for band III. Mixing of the electron states for the azulene moiety with those for the entire aromatic core is probably responsible for the change in the orientation of the vibronic transition moments for the azulene band as we move along the series I, II, III. This mixing should become more effective as the azulene and the shortwave bands for II and III (polarized along the long axis of the aromatic core) approach one another. Although the substituents do not significantly shift the azulene band, the shortwave bands shift appreciably (from 352 to 373 and 404 nm, see Fig. 1) and increase severalfold in intensity[9] as we go from I to II and III. This favors a larger polarization change for the shortwave vibronic transitions in the azulene band, in agreement with the spectral dependence $N(\lambda)$ for I and with the rapid rise in $N(\lambda)$ as λ decreases toward the shortwave edges of the bands for II and III or as we go from I to II, III (Fig. 1).

4. RELATION OF THE SPLITTING TO THE ELECTRON STRUCTURE AND ORIENTATIONAL ORDER OF THE MOLECULES

The intermolecular interactions may indirectly influence the electron structure and mix the electron states of the molecules by altering the molecular conformation, and hence also the degree of π-electron conjugation and the oscillator strengths for the electron transitions. Since the oscillator strength for the long-wave transition III is found to change[9] in the CHC mesophase, the relation of the splitting to the perturbations of the electron transition for the impurity molecule requires investigation. To answer this question we analyzed the spectra of impurities II and III in CHC and 5CB matrices, respectively. We verified that when band II was split, the oscillator strength

$$\frac{A_n}{K} = \frac{1}{\rho}\left(\frac{n_\|}{f_\|^2} D_\| + \frac{2n_\perp}{f_\perp^2} D_\perp\right) \qquad (7)$$

for the transition is independent of the phase of the CHC matrix and agrees with the value obtained from (1) using data for the isotropic phase.

For the 5CB matrix, the peaks in band III in the isotropic phase are shifted from 404 and 592 nm to 407 and 580 nm. This shift toward shorter wavelengths for the azulene III band in the more polar 5CB matrix is in accord with the results in Ref. 14 for pure azulene. Figure 3a shows the optical densities $D_{\|,\perp,i}$ corresponding to the peaks of the impuri-

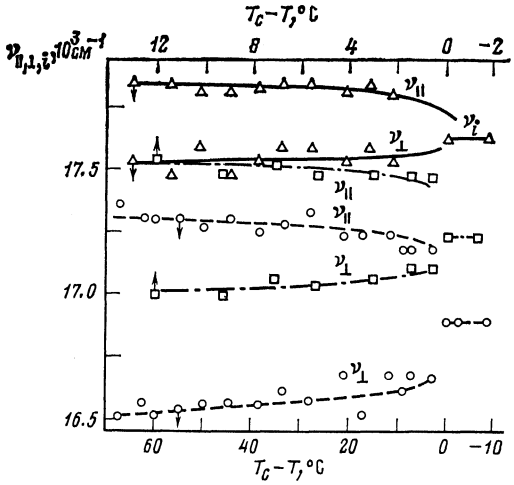

FIG. 4. Positions $\nu_{\|,\perp,i}$ of the peaks in the longwave polarized absorption bands as functions of temperature for impurities II (△) and III (○) in a CHC matrix and impurity III (□) in 5CB. The solid, dashed, and dashed-dotted curves were calculated using Eqs. (11) in the approximation $m = l = 0$.

ty band components in the nematic and isotropic phases of 5CB. The parameters Σ and $A_{n,i}$ for these bands were calculated using data on $n_{\|,\perp,i}$ in Ref. 10; $L_{\|,\perp}$ was found from the dashed curve in Fig. 3b in Ref. 11, and ρ was taken from Ref. 15. The temperature behavior of $D_\|$, $\bar{D} = (D_\| + 2D_\perp)/3$ in the mesophase and the relationship between $\bar{D}$ and D_i are markedly different for the two bands caused by impurity III. However, in both cases the ratio A_n/K is closely approximated by the dependence[9]

$$A_n = A_n(0)\,(1+\varkappa S_M^2), \tag{8}$$

where S_m is the order parameter for the matrix[11] (Fig. 3b). For the 407 and 580 nm bands, the values $A_n(0)/K = 3.81$ and 0.49 extrapolated to $S = 0$ agree with the experimental values $A_i/K = 3.68$ and 0.48, but $\varkappa$ is equal to 0.367 and 0.248, respectively. Comparison with previous data on $\varkappa$ in Ref. 9 reveals that for the 5CB matrix, the 580 nm transition is perturbed more strongly and the 407 nm transition less strongly than in a CHC matrix. Although this is consistent with the tendency of $|\varkappa|$ to increase as λ_{max} decreases,[9] the band splitting for III is less for 5CB than for CHC (Fig. 4). These results for II and III indicate that the band splittings are not correlated with perturbations of the electron transitions in the mesophase.

To interpret the experimental results, we first note that if a purely electronic transition contains closely spaced vibronic transitions with overlapping bands and different angles β, φ, the resultant absorption band may be structureless and the angles $\beta(\nu)$ and $\varphi(\nu)$ can be assumed to be continuous within the band. This situation is typical for the intrinsic absorption bands of liquid crystals and occurs for the azulene bands of impurities II and III.

For the transition for impurity III, the maximum difference between A_i and A_n is less than 10%; we may therefore neglect the dependence $A_n(S)$ in (1), which becomes

$$\begin{aligned} D_\|(\nu) &= D_i(\nu)\,[1+2SS_\beta(\nu) - {}^2/_3 G G_{\beta\varphi}(\nu)]/g_3(\nu), \\ D_\perp(\nu) &= D_i(\nu)\,[1-SS_\beta(\nu) + {}^1/_3 G G_{\beta\varphi}(\nu)]/g_2(\nu), \end{aligned} \tag{9}$$

where $D_{\|,\perp,i}(\nu)$ is the spectral distribution of the optical densities of the bands,

$$g_2(\nu) = \frac{\rho_i n_\perp}{\rho n_i}\left(\frac{f_i}{f_\perp}\right)^2, \qquad g_3(\nu) = \frac{\rho_i n_\|}{\rho n_i}\left(\frac{f_i}{f_\|}\right)^2.$$

The refractive index is relatively insensitive to wavelength near the impurity absorption bands, and the frequency dependence $g_{2,3}(\nu)$ can be neglected in a narrow frequency interval about the absorption peaks. The frequencies $\nu_{\|,\perp}$ corresponding to the peaks of the components polarized along and normal to the director are then given by the equations $dD_{\|,\perp}(\nu)/d\nu$, or

$$\begin{aligned} &D_i'(\nu) + 2S[D_i(\nu)S_\beta(\nu)]' - \frac{2G}{3}[D_i(\nu)G_{\beta\varphi}(\nu)]' = 0, \\ &D_i'(\nu) - S[D_i(\nu)S_\beta(\nu)]' + \frac{G}{3}[D_i(\nu)G_{\beta\varphi}(\nu)]' = 0. \end{aligned} \tag{10}$$

This shows that unlike band splitting due to resonant intermolecular interactions,[3-5,7] in this case the frequencies $\nu_{\|,\perp}$ are independent of the density, refractive index, and local field parameters of the liquid crystal and depend solely on the electron structure and orientational order of the molecules. To relate $\nu_{\|,\perp}$ to the position ν_i of the absorption peak in the isotropic phase, we expand the derivatives in (10) about $\nu = \nu_i$ and keep only terms linear in the small difference $\nu - \nu_i$. Equations (10) then have the solution

$$\begin{aligned} \nu_\| &= \nu_i + \frac{2(aS - mG/3)}{1 + 2(bS - lG/3)}, \\ \nu_\perp &= \nu_i - \frac{aS - mG/3}{1 - bS + lG/3}, \end{aligned} \tag{11}$$

where

$$\begin{aligned} a &= S_\beta'(\nu_i)/\alpha, \qquad m = G_{\beta\varphi}'(\nu_i)/\alpha, \\ \alpha &= |D_i''(\nu_i)|/D_i(\nu_i), \qquad b = S_\beta(\nu_i) - S_\beta''(\nu_i)/\alpha, \\ l &= G_{\beta\varphi}(\nu_i) - G_{\beta\varphi}''(\nu_i)/\alpha. \end{aligned} \tag{12}$$

Here the primes denote derivatives at the point $\nu = \nu_i$. According to (11), the derivatives $S_\beta'(\nu_i)$ and $G_{\beta\varphi}'(\nu_i)$ determine the sign of the splitting $\Delta\nu = \nu_\| - \nu_\perp$, and $|\Delta\nu|$ is larger for bands with sharper peaks (small α) and increases with S, in qualitative agreement with experiment (Figs. 1, 4).

For a quantitative comparison, we note that $\varphi \approx 45°$ for the vibronic transition responsible for the absorption maxima for impurities I–III. Therefore, the spectral behavior of N (Fig. 1) implies that the dependence $S_\beta(\nu)$ is linear near the peaks for II and III, and $S_\beta''(\nu_i) \approx 0$. Moreover, since $S \gg G/3$ and $G_{\beta\varphi}(\nu_i) \approx 0$ for the long molecules II, III, the corresponding terms in (11) can be neglected and we may set $b = S_\beta(\nu_i)$. We calculated the temperature dependences $\nu_{\|,\perp}(\Delta T)$ from (11) by using values $\Sigma = S$ taken from Ref. 9 for the 373 (II) and 404 (III in CHC) transitions and the values in Fig. 3a for the 407 nm transition (III in 5CB). We chose a and b to give the best fit with the experimental values of $\nu_{\|,\perp}$ for $\Delta T = 39°$ (II), 55° (III in CHC), and 3 °C (III in 5CB). We see from Fig. 4 that subject to the above approximations, Eqs. (11) accurately describe the temperature dependence $\nu_{\|,\perp}(\Delta T)$ throughout the mesophase interval.

The band splitting data for impurity II give $b \approx 0$, which implies that $\beta(\nu_i) = 55°$, in good agreement with the above

independent estimate $\beta \approx 53°$ based on the dichroism data. The values $a = 712\ \text{cm}^{-1}$ and $b = 0.517$ for impurity III in CHC may be compared with $a = 398\ \text{cm}^{-1}$ and $b = 0.326$ in 5CB. We find that $\beta(\nu_i) = 35°$ and 42°, in agreement with the above estimate $\beta \approx 40°$ from the dichroism data. As expected, the intramolecular parameter β is insensitive to intermolecular interactions (in particular, to the polarity of the matrix). The value of a is lower for 5CB than for CHC because α is larger due to the increase in $|D_i''(\nu_i)|$ (the band extinction coefficient increases by 40%). This explains why the splitting of the III band is weaker in 5CB (Fig. 4). The measured dichorism and band splittings thus provide a mutually consistent description of the electron structure of the impurity molecules.

The dependences $\nu_{\|,\perp}(S)$ have some distinctive features. For $m = l = 0$, the qualitative behavior $\nu_{\|,\perp}(S)$ is determined by $\beta(\nu_i)$. When $\beta(\nu_i) = \beta_m$, the shifts $\Delta\nu_\| = \nu_\| - \nu_i$ and $\Delta\nu_\perp = \nu_i - \nu_\perp$ in the absorption peaks depend linearly on S, and $\Delta\nu_\| = 2\Delta\nu_\perp$. There is a large anisotropy $\Delta\nu_\| \gg \Delta\nu_\perp$ when $\beta(\nu_i) > \beta_m$, particularly for large S. Moreover, the dependence $\Delta\nu_\perp(S)$ is almost linear, while $\Delta\nu_\|(S)$ is highly nonlinear. For $\beta(\nu_i) \leqslant 45°$ there exists a value $S = S^* = S_\beta/4$ at which $\Delta\nu_\| = \Delta\nu_\perp$, and $\Delta\nu_\| < \Delta\nu_\perp$ for $S > S^*$, $\Delta\nu_\| > \Delta\nu_\perp$ for $S < S^*$. This case corresponds to the experimental data for III in CHC (Fig. 4). As $S \to 0$, the dependences $\Delta\nu_{\|,\perp}(S,\beta)$ approach $\Delta\nu_{\|,\perp}(S,\beta_m)$.

If one or more sharp peaks are present in the envelope of the vibronic series of overlapping bands (as for band I in Fig. 1), their positions for the $\|$ and $\perp$ polarizations may coincide because α in (12) is large while a and m are small. However, even in this case the centroids of the $\|$ and $\perp$ components of the envelope will differ. The centroids $\bar\nu_{\|,\perp}, \bar\nu_i$ of the polarization components in the mesophase and in the isotropic liquid are given by

$$\bar\nu_{\|,\perp,i} = \int \nu D_{\|,\perp,i}(\nu)\,d\nu \Big/ \int D_{\|,\perp,i}(\nu)\,d\nu, \qquad (13)$$

where the integration is over the entire envelope of the band. If we can neglect the frequency-dependence of the parameters $g_{2,3}(\nu)$ in (9), then $\bar\nu_{\|,\perp,i}$ will be independent of the refractive indices of the liquid crystal and the corrections to the local field. Equation (13) leads to reasonably simple expressions for $\bar\nu_{\|,\perp}(S,G)$ only if the functions $S_\beta(\nu)$ and $G_{\beta\varphi}(\nu)$ are nearly linear over the entire vibronic series. In this case we can relate $\bar\nu_{\|,\perp}$ to $\bar\nu_i$ by substituting $D_{\|,\perp}(\nu)$ from (9) into (13), expanding $S_\beta(\nu)$ and $G_{\beta\varphi}(\nu)$ about $\nu = \bar\nu_i$, and keeping linear terms. The resulting formulas for $\bar\nu_{\|,\perp}$ are similar to (11), with

$$\begin{aligned} &a = S_\beta'(\bar\nu_i)\,\delta_\nu, \qquad m = G_{\beta\varphi}'(\bar\nu_i)\,\delta_\nu, \\ &\delta_\nu = \overline{\nu^2} - \bar\nu_i^2, \qquad b = S_\beta(\bar\nu_i), \qquad l = G_{\beta\varphi}(\bar\nu_i). \end{aligned} \qquad (14)$$

Since $\delta_\nu > 0$, for $S \gg G/3$ the sign of the splitting $\Delta\bar\nu = \bar\nu_\| - \bar\nu_\perp$ is determined by the sign of the derivative $S_\beta'(\bar\nu_i)$, while its magnitude increases with the width of the band and hence with $\delta\nu$. $\bar\nu_{\|,\perp}(S)$ depends on $\beta(\bar\nu_i)$ in the same way as the positions of the peaks $\nu_{\|,\perp}(S)$ considered above. In principle, one can find the parameter $\beta(\bar\nu_i)$ by a best-fit analysis of the theoretical and experimental curves $\bar\nu_{\|,\perp}(S)$. However, the assumptions used to derive Eqs. (11) are justified only in a small neighborhood of the band peaks and not throughout the entire bands. For weakly asymmetric bands with a single peak (as for impurity III, see Fig. 1), it is therefore preferable to compare the calculated and experimental positions of the band peaks $\nu_{\|,\perp}(S)$ rather than the centroids. Figure 4 and the agreement in the parameters $\beta(\nu_i)$ show that Eqs. (11) also accurately approximate the experimental results for impurity II, whose absorption band is appreciably asymmetric.

In closing we note that the absorption band splitting mechanism studied above is independent of the specific properties of the liquid-crystal state and should also be observed in oriented polymer films, LC polymers, surface-active layers, molecular gases oriented by an external field, and other isotropic systems.[16] Due to the higher degree of molecular alignment for impurity III (S may reach values $S \approx 0.8$ typical of smectic matrices or vitrified nematics LC's), the band splitting can be as large as $\Delta\nu \approx 1500\ \text{cm}^{-1}$. Because appropriate orienting matrices can be found and the electron structure of the azulene derivatives can be adjusted by changing the substituents, these materials should prove useful as impurities in applications that employ an external field to reorient the director and achieve continuously adjustable spectral properties.

[1] L. M. Blinov, Élektro- i Magnetooptika Zhidkikh Kristallov (Electro- and Magnetooptics of Liquid Crystals), Nauka, Moscow (1978), Chap. 2, p. 43; Chap. 4, p. 148.
[2] V. K. Dolganov, Fiz. Tverd. Tela **19**, 3269 (1977) [Sov. Phys. Solid State **19**, 1910 (1977)].
[3] E. M. Aver'yanov, Fiz. Tverd. Tela **22**, 1867 (1980) [Sov. Phys. Solid State **22**, 1088 (1980)].
[4] V. I. Sugakov and S. V. Shiyanovskiĭ, Fiz. Tverd. Tela **22**, 901 (1980) [Sov. Phys. Solid State **22**, 527 (1980)]; Opt. Spektrosk. **48**, 542 (1980) [Opt. Spectrosc. (USSR) **22**, 298 (1980)].
[5] S. V. Shiyanovskiĭ, Ukr. Fiz. Zh. **26**, 137 (1981).
[6] L. M. Blinov, V. A. Kizel', V. G. Rumyanstsev, and V. V. Titov, Kristallograf. **20**, 1245 (1975) [Sov. Phys. Crystallogr. **20**, (1975)].
[7] V. S. Libov and A. Yu. Tikhomirov, Opt. Spectrosc. **56**, 631 (1984) [Opt. Spectrosc. (USSR) **56**, 386 (1984)].
[8] V. G. Rumyantsev, V. M. Muratov, V. A. Churkina, T. N. Rumyantseva, V. T. Grachev, V. V. Titov, and V. A. Nefedov, in: Proc. Fifth Conf. Socialist Countries on Liquid Crystals, Vol. 1, Odessa (1983), p. 142.
[9] E. M. Aver'yanov, V. M. Muratov, and V. G. Rumyantsev, Zh. Eksp. Teor. Fiz. **88**, 810 (1985) [Sov. Phys. JETP **61**, 476 (1985)].
[10] E. M. Aver'yanov, V. Ya. Zyryanov, V. A. Zhuĭkov, and Yu. I. Ruolene, Zh. Struk. Khim. **24**(5), 101 (1983).
[11] E. M. Aver'yanov, V. A. Zhuĭkov, V. Ya. Zyryanov, and V. F. Shabanov, Zh. Eksp. Teor. Fiz. **86**, 2111 (1984) [Sov. Phys. JETP **59**, 1227 (1984)].
[12] E. Helbronner, in: Nebenzoidnye Aromaticheskie Soedineniya (Nonbenzoid Aromatic Compounds), translated from the English by A. N. Nesmeyanov, IL, Moscow (1963), Chap. 5, p. 176.
[13] E. M. Aver'yanov, P. V. Adomenas, V. A. Zhuĭkov, and V. Ya. Zyryanov, Fiz. Tverd. Tela **24**, 28 (1982) [Sov. Phys. Solid State **24**, 15 (1982)].
[14] W. W. Robertson, A. D. King, and O. E. Weigang, J. Chem. Phys. **35**, 464 (1961).
[15] D. A. Dunmur and W. H. Miller, J. de Phys., Colloq. C3, **40**, C3-141 (1979).
[16] B. Norden, Spectr. Lett. **10**, 381 (1977).

Translated by A. Mason